Band-gap shift and defect-induced annihilation in prestressed elastic structures

M. Gei,[1,a] A. B. Movchan,[2] and D. Bigoni[1]
[1]*Department of Mechanical and Structural Engineering, University of Trento, Via Mesiano 77, I-38050 Trento, Italy*
[2]*Department of Mathematical Sciences, University of Liverpool, Liverpool L69 3BX, United Kingdom*

(Received 18 November 2008; accepted 28 January 2009; published online 18 March 2009)

Design of filters for electromagnetic, acoustic, and elastic waves involves structures possessing photonic/phononic band gaps for certain ranges of frequencies. Controlling the filtering properties implies the control over the position and the width of the band gaps in question. With reference to piecewise homogeneous elastic beams on elastic foundation, these are shown to be strongly affected by prestress (usually neglected in these analyses) that (i) "shifts" band gaps toward higher (lower) frequencies for tensile (compressive) prestress and (ii) may "annihilate" certain band gaps in structures with defects. The mechanism in which frequency is controlled by prestress is revealed by employing a Green's-function-based analysis of localized vibration of a concentrated mass, located at a generic position along the beam axis. For a mass perturbing the system, our analysis addresses the important issue of the so-called effective negative mass effect for frequencies within the stop bands of the unperturbed structure. We propose a constructive algorithm of controlling the stop bands and hence filtering properties and resonance modes for a class of elastic periodic structures via prestress incorporated into the model through the coefficients in the corresponding governing equations. © *2009 American Institute of Physics*. [DOI: 10.1063/1.3093694]

I. INTRODUCTION

Periodic structures, for instance, phononic and photonic crystals,[1] are known to display important filtering properties for electromagnetic, acoustic, and elastic waves: the so-called band gaps (BGs) (frequency ranges where the waves are evanescent),[2–5] localized or defect modes (an exponentially localized waveform located near a periodicity-breaking element),[6,7] negative refraction (refraction occurring on the same side of the normal to the interface where the incoming wave is incident),[8–12] and effective negative mass effects (corresponding to an exponential decay of vibrational modes rather than sinusoidal propagation).[13–15] Elastic waves are addressed in this article, which are the key to vibration control of structural systems and to the design of signal transmission properties in sensors.[16]

In the field of elastic structural systems (beams, plates, and shells, namely the basic models of mechanical design), analyses of BGs date back to Cremer and Leilich,[23] Miles,[24] and Lin,[25] and, later, to Mead.[26,27] In the recent papers by Yu *et al.*[28,29] flexural systems with BG properties were addressed; these included analysis of Euler–Bernoulli beams with locally resonant structures as well as flexural vibration BGs in Timoshenko beams.

In general, elastic periodic systems have been analyzed from a number of perspectives. In particular, Movchan and co-workers[30–32] developed the asymptotic methods for the resonance modes in question. It is also noted that the prestress changes the dispersion properties of Bloch–Floquet elastic waves within periodic systems, but the analytical studies of prestress—coupled to periodicity—have never been explicitly addressed for flexural Bloch–Floquet waves within inhomogeneous periodic elastic systems.[33]

Flexural wave propagation in a piecewise homogeneous elastic beam on an elastic foundation (of Winkler type; see Ref. 38) and prestressed by a uniform (tensile or compressive) axial force is considered in the present article. In addition, the presence of defects[39] in the form of cracks partially cutting the beam is modeled by effective rotational springs, so that the bending moment remains continuous, but the rotation angle has a jump across the junction.

The practical applications of prestressed structures have been addressed in a number of experimental works. In particular, a cantilever beam prestressed near buckling has been considered in Ref. 41 and, with regard to micromechanics, highly stressed silicon microresonators have been investigated in Refs. 42 and 43.

Along with the analysis of Bloch–Floquet waves within a periodic and prestressed elastic system, we address the important issues of localization, and, in particular, a problem of localized mass perturbation along the beam is solved through a Green's function approach, exploiting the recent findings of Movchan and Slepyan[7] on lattice structures. The investigation shows the strong influence of prestress on the filtering properties of flexural phononic BG structures, and we specifically address the following features:

(i) The prestress controls the frequency location of the BGs. A shift toward high (low) frequency is revealed when tensile (compressive) prestress is applied.
(ii) The prestress can eliminate or, say, "annihilate," certain BGs in defected structures.
(iii) Defect modes and effective negative mass effects[44] are analyzed with the emphasis on their strong sensitivity with regards to the prestress.

[a]Author to whom correspondence should be addressed. Tel.: +39-0461-882523. FAX: +39-0461-882599. Electronic mail: mgei@ing.unitn.it.

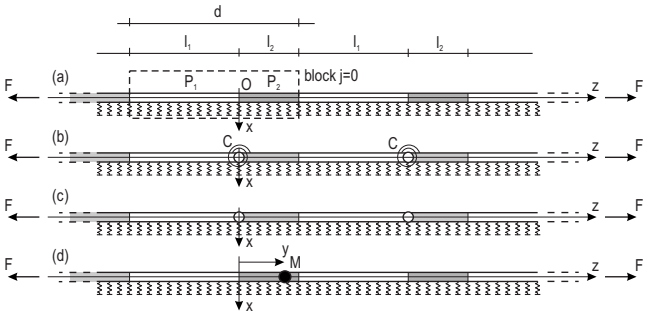

FIG. 1. Sketches of the piecewise homogeneous beam on an elastic foundation (visualized as a distribution of springs) studied in the paper: (a) perfect structure, (b) structure with localized defects transmitting bending moments across the damaged sections (which depend linearly on the rotation angle jumps; C is the stiffness of the rotational springs), (c) structure with localized defects of hinge type across the damaged sections ($C=0$), and (d) perfect structure with additional mass M placed at $z=y$. F represents the longitudinal prestress.

The present paper provides a definitive answer to the modeling of controlled BG structures responding to flexural vibrations. The new properties of solutions disclose a new approach to the design of efficiently controlled elastic wave filters and polarizers.

II. BAND-GAP SHIFT FOR PERIODIC FLEXURAL SYSTEMS

Following the results of the asymptotic analysis of Bigoni *et al.*,[34] we use the "beam approximations" to model the Bloch–Floquet flexural waves within prestressed periodic beams on an elastic foundation of the Winkler type; it is assumed that the typical wavelength is much larger compared to the thickness of the structure itself. The elastic stiffness of the foundation for the model considered here can be related to the properties of the corresponding half space as discussed in Ref. 34. The periodic geometry is shown in Fig. 1, where F denotes the longitudinal prestress applied at infinity. The period is equal to d, and in the unperturbed (*perfect*) structure, consisting of two types of materials and shown in Fig. 1(a), the interface conditions of ideal contact incorporate continuity of the displacement, the angle of rotation, as well as the continuity of the transverse forces and bending moments. Furthermore, periodically distributed "defects" are introduced by incorporating imperfect junction conditions [see the rotational springs in Fig. 1(b) or the hinge-type junctions in Fig. 1(c)]. The periodicity can be broken by the addition of a mass into the central cell of the structure [as in Fig. 1(d)] without affecting the physical characteristics of other cells; in this way, an exponentially localized waveform can be constructed for a certain frequency range.

For each of the phases m within the periodic structure, the time harmonic flexural displacement $w_m(z)$ satisfies the following governing equation:

$$B_m w_m'''' - F w_m'' + (S - \rho_m \omega^2) w_m = 0 \quad (m = 1,2), \tag{1}$$

where ρ_m are the values of the piecewise constant mass density $\rho(z)$, $B(z)=I(z)E(z)$ is the bending stiffness [with the second-order moment $I(z)$ and the Young modulus $E(z)$], and the stiffness of the elastic foundation is denoted by S (see Refs. 45 and 46 for details on the nomenclature).

The flexural displacements are sought in the form

$$w_m = \xi_m \exp(ik^{(m)} z) \quad (m = 1,2). \tag{2}$$

The substitution of Eq. (2) into Eq. (1) yields the following equations for the circular frequency ω:

$$(k^{(m)} r_m)^4 + \bar{F}_m (k^{(m)} r_m)^2 + \bar{S}_m - P_m \omega^2 = 0 \quad (m = 1,2), \tag{3}$$

where the following dimensionless parameters have been introduced:

$$\bar{F}_m = \frac{F r_m^2}{B_m}, \quad \bar{S}_m = \frac{S r_m^4}{B_m} \quad (m = 1,2), \tag{4}$$

in which r_m are the radii of inertia of the beam cross section, while

$$P_m = \frac{\rho_m r_m^4}{B_m} \quad (m = 1,2) \tag{5}$$

have the dimension of a squared time. The quantities r_m are related to the second-order moments I_m and the cross-sectional areas A_m of the beam by

$$r_m = \sqrt{I_m / A_m} \quad (m = 1,2).$$

Equation (3) provides the following eight solutions:

$$k_{1,2,3,4}^{(m)} = \pm \frac{1}{r_m} \sqrt{-\frac{\bar{F}_m}{2} \pm \sqrt{\frac{\bar{F}_m^2}{4} + P_m \omega^2 - \bar{S}_m}} \quad (m = 1,2), \tag{6}$$

so that the transverse displacements w_1, w_2 become a linear combination of four terms, namely,

$$w_1(z) = \sum_{p=1}^{4} \xi_1^p \exp(ik_p^{(1)} z), \quad w_2(z) = \sum_{p=1}^{4} \xi_2^p \exp(ik_p^{(2)} z). \tag{7}$$

The eight constants of the problem can be obtained by imposing the interface conditions at the internal interface of the elementary block. For a *perfect structure* [shown in Fig. 1(a)], these are continuity of displacement, rotation, bending moment, and shear force, so that, for the block $j=0$, the interface is located at $z=0$ and the corresponding interface conditions for the functions w_1, w_2 and their derivatives are

$$w_1(0) = w_2(0), \quad w_1'(0) = w_2'(0),$$

$$B_1 w_1''(0) = B_2 w_2''(0), \quad B_1 w_1'''(0) = B_2 w_2'''(0). \tag{8}$$

For a *defected structure*, where a crack partially cuts the cross section of the beam, a rotational elastic spring of stiffness C is introduced to link the two points across the damaged section of the beam [Fig. 1(b)] (see Ref. 47 for an estimation of C in terms of the ratio between cracked and total cross section areas). Here the rotation of the axis of the beam is no longer continuous and the condition (8) is substituted by the constitutive equation of the spring. For $j=0$, at $z=0$, condition (8) now becomes

$$w_1(0) = w_2(0), \quad w_2'(0) - w_1'(0) = \frac{B_1}{C} w_1''(0),$$

$$B_1 w_1''(0) = B_2 w_2''(0), \quad B_1 w_1'''(0) = B_2 w_2'''(0). \tag{9}$$

The remaining four equations follow from imposition of the *Bloch–Floquet conditions*, linking fields at the boundaries of the elementary block, namely,

$$w_2(l_2^-) = w_1(-l_1^+)\exp(iKd), \quad w_2'(l_2^-) = w_1'(-l_1^+)\exp(iKd), \tag{10}$$

$$B_2 w_2''(l_2^-) = B_1 w_1''(-l_1^+)\exp(iKd),$$

$$B_2 w_2'''(l_2^-) = B_1 w_1'''(-l_1^+)\exp(iKd), \tag{11}$$

where K is the Bloch parameter. Equations (8)–(11) provide a homogeneous system for the eight unknown constants ξ_1^p, ξ_2^p $(p=1,\ldots,4)$, so that the vanishing of the determinant of the associated matrix yields the dispersion equation of the system. We note that if ω is taken to be zero in Eqs. (1) and (6), the system (8)–(11) provide the buckling load of the structure.[45,48]

A. Results for a perfect structure

Solutions to the dispersion equation relative to a perfect beam [Fig. 1(a)] with piecewise constant mass density $(\rho_1 \neq \rho_2)$, but uniform bending stiffness $(B_1=B_2$, yielding $\bar{F}_1=\bar{F}_2=\bar{F})$, are reported in Fig. 2 for $P_2/P_1=0.1$, $\bar{S}=0.0001$, $r/d=0.015$, $l_1=l_2=d/2$, and three different levels of prestress $\bar{F}$ [tensile, null, and compressive in Figs. 2(a)–2(c), respectively]. For this beam, the buckling force corresponds to $\bar{F}_{\text{buckl}}=-0.02$, while the cutoff frequency of the homogeneous counterpart—which can be recovered if $P_1=P_2$—is $\sqrt{P_1}\omega_0=0.01$.

At a given dimensionless circular frequency $\sqrt{P_1}\omega$, four complex values of the Bloch parameter K can be found from the dispersion equation, which occur in positive and negative pairs. In particular, a propagating mode corresponds to a pure real K, while a monotonic decaying mode is found when K is purely imaginary; for complex conjugate Bloch parameters, the mode also does not propagate and decays sinusoidally.

For each value of prestress $\bar{F}$, two diagrams are displayed in Fig. 2, namely, the dimensionless parameters $\text{Im}(K)d$ and $\text{Re}(K)d$ on the left and on the right, respectively. Both diagrams are symmetric with respect to the vertical axis $K=0$, so that only the positive ranges have been plotted. In the left parts of the figures, the solid lines denote purely imaginary solutions, $\text{Re}(K)=0$, while dashed lines correspond to complex solutions with $\text{Re}(K)=\pi/d$. The BG frequency ranges are marked with black segments. Note that in Figs. 2(b) and 2(c) and for $\sqrt{P_1}\omega<0.0094$ and 0.0042, respectively, K assumes complex conjugate values and results have been omitted for this type of solutions, which correspond to sinusoidally decaying modes.

The BG distribution is reported as a function of the prestress for fixed contrast parameter $P_2/P_1=0.1$ in Fig. 3(a), while a fixed, small, and tensile prestress is assumed in Fig. 3(b) for varying P_2/P_1. The latter figure makes evident that the cutoff region is not strongly influenced by the contrast parameter P_2/P_1 and that the range where the increase in the size of the BG zones is more pronounced occurs for $0.464<P_2/P_1<0.0464$.

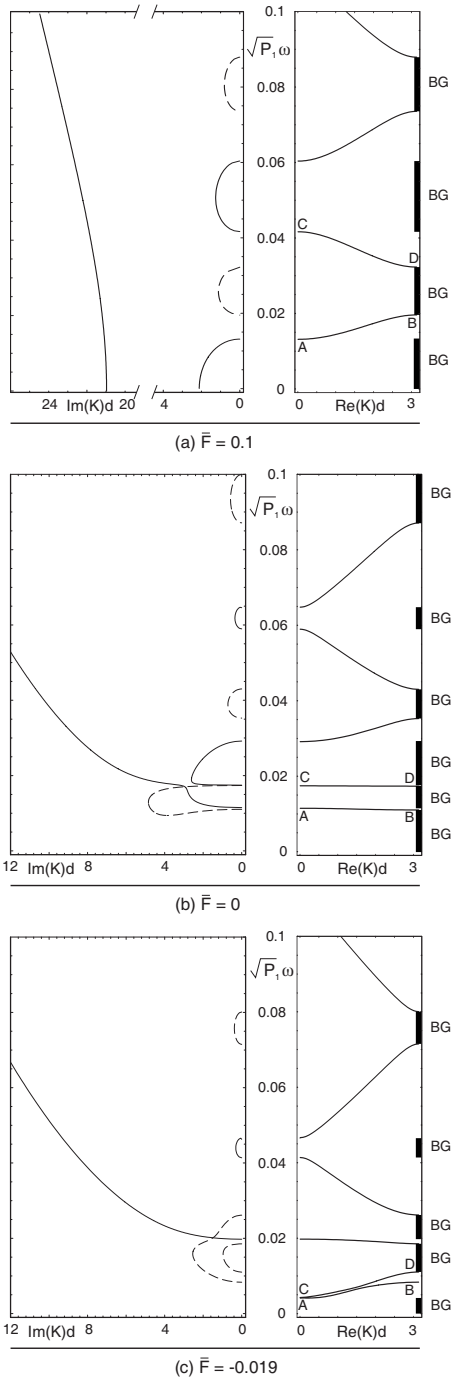

FIG. 2. Dispersion diagrams [circular frequency $\sqrt{P_1}\omega$ vs Bloch parameter $\text{Re}(K)d$ and $\text{Im}(K)d$] for a beam on an elastic foundation with piecewise constant mass density [Fig. 1(a)] and homogeneous flexural stiffness, $B_1=B_2$ $(P_2/P_1=0.1$, $\bar{S}=0.0001$, $r/d=0.015$, and $l_1=l_2=d/2)$. (a) Tensile prestress: $\bar{F}=0.1$. (b) Null prestress: $\bar{F}=0$. (c) Near-buckling $(\bar{F}_{\text{buckl}}=-0.02)$ compressive prestress: $\bar{F}=-0.019$. $\text{Im}(K)d$ is reported with a solid (dashed) line when $\text{Re}(K)=0$ $[\text{Re}(K)d=\pi]$. Note that in cases (b) and (c) for $\sqrt{P_1}\omega<0.0094$ and 0.0042, respectively, where solutions are not reported, K assumes complex conjugate values. BG denotes a band gap. Note that the compressive stress in (c) induces the annihilation of the second band gap (between branches AB and CD).

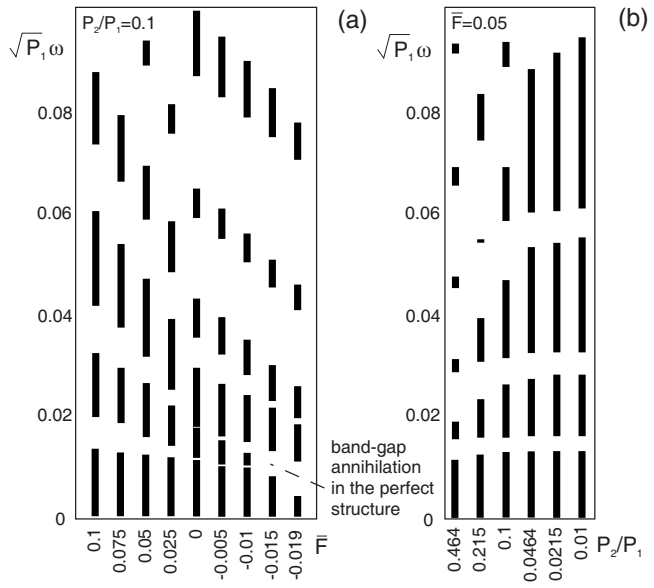

FIG. 3. Band gap/pass band distribution of a beam on an elastic foundation with piecewise constant mass density and homogeneous flexural stiffness, $B_1=B_2$ ($\bar{S}=0.0001$, $r/d=0.015$, and $l_1=l_2=d/2$): (a) in terms of prestress $\bar{F}$ ($P_2/P_1=0.1$) and (b) in terms of the contrast parameter P_2/P_1 (logarithmic scale) ($\bar{F}=0.05$). The band-gap annihilation induced by a compressive force is highlighted.

Let us consider now the two lower frequency BGs in Figs. 2 and 3(a), one of which is present also in a homogeneous beam on an elastic foundation. The prestress strongly modifies the BG intervals (shifting these toward higher frequencies for tensile loading) and, when this becomes compressive, the higher frequency BG (between branches AB and CD in Fig. 2) is reduced in size and *annihilated already before the buckling load is attained* (see Appendix for the calculation of the buckling load of a periodic beam).

B. Results for a structure with a periodic distribution of defects

In the case of an infinite piecewise homogeneous beam on an elastic foundation with defects localized at the internal interface of the periodicity cell, we have to impose boundary conditions (9)–(11) to obtain the dispersion equation.

A BG annihilation region—evidenced in gray—is shown in Fig. 4(a), where the dimensionless rotational spring stiffness has been introduced

$$\bar{C} = Cr/B_1, \tag{12}$$

and is reported versus the dimensionless prestress $\bar{F}$ defined earlier in Eq. (4). For a beam with rectangular cross section of height h and width b and through-width rectangular-shape crack of depth a, a physical interpretation of the degree of damage described by Eq. (12) can be inferred using the approach by Chondros *et al.*,[47] which estimates the effective rotational spring stiffness C in terms of factor a/h, reported on the vertical axis of Fig. 4(a). In the case of Fig. 4(a), where $B_1=B_2$, as $r=h/2\sqrt{3}$ for a rectangle, it turns out that

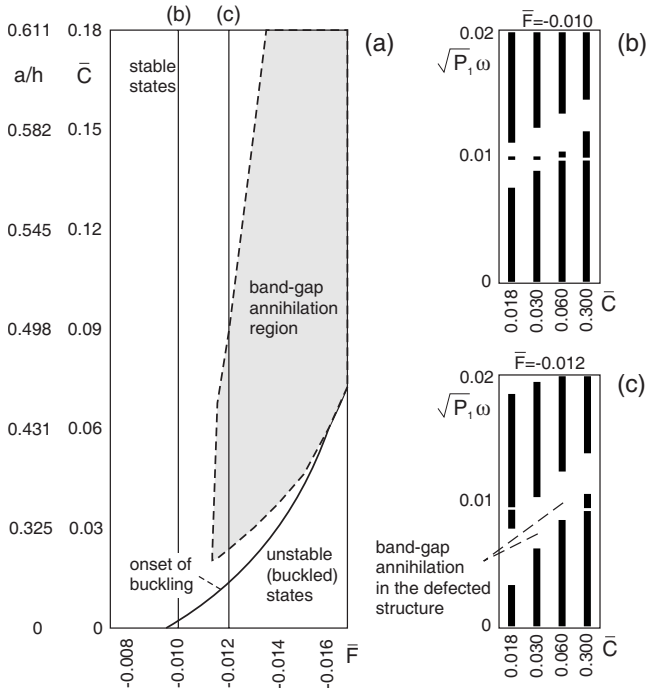

FIG. 4. (a) BG annihilation region in the diagram presenting the dimensionless rotational spring stiffness ($\bar{C}$) vs prestress ($\bar{F}$). For a beam with rectangular cross section of height h and width b and through-width rectangular-shape crack of depth a, the scale a/h corresponding to $\bar{C}$ is reported. (b) and (c) BG distributions for different compressive prestress forces ($P_2/P_1=0.1$, $B_1=B_2$, $\bar{S}=0.0001$, $r/d=0.015$, and $l_1=l_2=d/2$).

$$\bar{C} = \frac{1}{12\sqrt{3}\pi(1-\nu^2)\Phi(a/h)}, \tag{13}$$

where $\Phi(a/h)$ is a polynomial function.[49] The black lines in the diagram correspond to the BG distributions shown in Figs. 4(b) and 4(c) plotted for two representative values of compressive prestress. We highlight in Fig. 4(a) the effect of a compressive force in the beam that induces dramatic changes in the dynamic behavior when compared to that of a tensile force, leaving the response qualitatively unchanged. The line corresponding to the onset of buckling separates stable configurations from unstable—buckled—states. The point of intersection of this line with the axis $\bar{C}=0$ (at $\bar{F}=-0.00959$) is representative of the buckling load of a periodic beam with hinges at the internal interface of the periodic cell [Fig. 1(c)].

III. BAND-GAP LOCALIZED MODES AND EFFECTIVE NEGATIVE MASS EFFECTS

The strong influence of prestress F on "localized defect modes" present within the BG frequencies is demonstrated for an infinite piecewise uniform beam on an elastic foundation, making use of a Green's function formulation. The case of piecewise constant properties is postponed to the treatment of the uniform beam, which can be analytically solved.

In the range of a forbidden frequency, say, $0<\omega<\omega_{\min}$, a localized mode can be created by an oscillating point mass, inserted at a point of the (for the moment homogeneous) beam. In order to arrive at the mass-frequency relationship,

the time-harmonic Green's function $\hat{g}(z,y;t) = g(z,y)\exp(i\omega t)$ has to be obtained for the unit force placed at $z=y$. For this purpose, we introduce the parameters

$$\alpha = -\frac{\bar{F}}{2r^2}, \quad \beta = \sqrt{\frac{1}{r^4}\left(\frac{\bar{F}^2}{4} + P\omega^2 - \bar{S}\right)}, \tag{14}$$

so that α is real and β is purely imaginary, to correspond to a stationary wave. The four solutions (6) now become

$$k_{1,2} = \mp\sqrt{\alpha - \beta}, \quad k_{3,4} = \mp\sqrt{\alpha + \beta}. \tag{15}$$

An admissible form for $g(z,y)$, satisfying decaying conditions at $|z| \to \infty$, is

$$g(z,y) = C^1 \exp[ik_1(z-y)] + C^4 \exp[ik_4(z-y)]. \tag{16}$$

Let us introduce the notation $k_1 = -\sqrt{\alpha-\beta} = -\hat{\alpha} + i\hat{\beta}$ and $k_4 = \sqrt{\alpha+\beta} = \hat{\alpha} + i\hat{\beta}$, where $\hat{\alpha}$ and $\hat{\beta}$ are real. The square-root rule for a complex number gives

$$\hat{\alpha} = \frac{1}{2r}\sqrt{-\bar{F} + 2\sqrt{\bar{S} - P\omega^2}}, \quad \hat{\beta} = \frac{1}{2r}\sqrt{\bar{F} + 2\sqrt{\bar{S} - P\omega^2}}, \tag{17}$$

therefore

$$\hat{\alpha}^2 + \hat{\beta}^2 = \frac{1}{r^2}\sqrt{\bar{S} - P\omega^2}. \tag{18}$$

Therefore, the Green's function writes (similar to Ref. 7)

$$g(z,y) = \frac{e^{-\hat{\beta}|z-y|}}{4B(\hat{\alpha}^2 + \hat{\beta}^2)}\left(\frac{\sin\hat{\alpha}|z-y|}{\hat{\alpha}} + \frac{\cos\hat{\alpha}(z-y)}{\hat{\beta}}\right), \tag{19}$$

where $\hat{\beta}$ is the localization exponent, which is now positive, or, in other words, to a solution formally corresponding to vibrations of a system involving an *effective negative mass*, and hence exponentially vanishing (as described by Milton and Willis[15]).

Let us consider now a concentrated mass M attached to the beam at the origin ($y=0$) and vibrating at a frequency $\omega < \omega_{\min}$. A concentrated force at $y=0$ is replaced by the inertial force of the mass M, which is equal to $M\omega^2 U$, where U is the amplitude. Since at $z=0$, $g(0,0)=U$, we obtain the mass-frequency equation

$$M = \frac{4B(\hat{\alpha}^2 + \hat{\beta}^2)\hat{\beta}}{\omega^2} = \frac{2B\sqrt{\bar{S} - P\omega^2}\sqrt{\bar{F} + 2\sqrt{\bar{S} - P\omega^2}}}{r^3\omega^2}, \tag{20}$$

where the prestress contribution ($\bar{F}$) is made explicit or, alternatively,

$$\bar{M}P\omega^2 - B\sqrt{\bar{S} - P\omega^2}\sqrt{\bar{F} + 2\sqrt{\bar{S} - P\omega^2}} = 0, \tag{21}$$

where

$$\bar{M} = \frac{M}{2\rho r}. \tag{22}$$

The above formula, together with Eq. (20), gives the value of an additional mass required to support a localized vibration mode of frequency $\omega < \omega_{\min}$. If a periodic set of masses is introduced for the infinite beam under prestress, then a narrow pass band, corresponding to waves of low group velocity, will appear and "break" the initial BG.

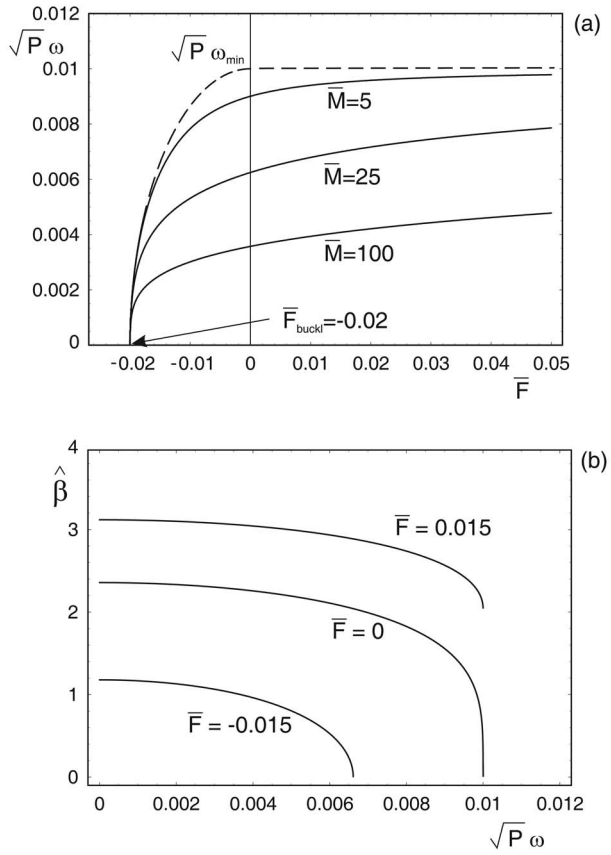

FIG. 5. (a) Vibrating frequency ω (normalized through multiplication by $\sqrt{P}$) of an oscillating unit point mass attached to an infinite, homogeneous, prestressed beam on an elastic foundation [Eq. (21)] as a function of the prestress $\bar{F}$ ($\bar{S}$=0.0001). Different dimensionless masses $\bar{M}$ ($\bar{S}$=0.0001) are considered. The upper boundary of the BG region at given $\bar{F}$ is reported with a dashed line. (b) Localization exponent $\hat{\beta}$ for three different prestress levels within the BG range. For $\bar{F}$=0.015, $\hat{\beta}$=2.04124 at the upper boundary of the BG range (i.e., $\sqrt{P}\omega$=0.01), while for the other two prestresses, $\hat{\beta}$ vanishes in the same limit.

Equation (21) shows that for a negative prestress force $\bar{F}$, the circular frequency may vanish, and this corresponds to the achievement of the buckling load.

The relationship between the dimensionless frequency $\sqrt{P}\omega$ and the prestress $\bar{F}$ at constant $\bar{M}$ is represented graphically in Fig. 5(a) for $\bar{S}$=0.0001, while the amplitude of vibration modes [normalized through division by $g(0,y)$] is reported in Fig. 6 along the beam axis for different prestress forces $\bar{F}$.

We note from Figs. 5 and 6 that a compressive prestress does influence significantly the vibration frequency of a given mass, especially near the buckling state, and that for $\bar{M} \to 0$ the frequency achieves the limit $\omega \to \omega_{\min}$. Moreover, a negative, i.e., compressive (positive, i.e., tensile) prestress strongly decreases (increases) the rate of localization of the vibration mode.

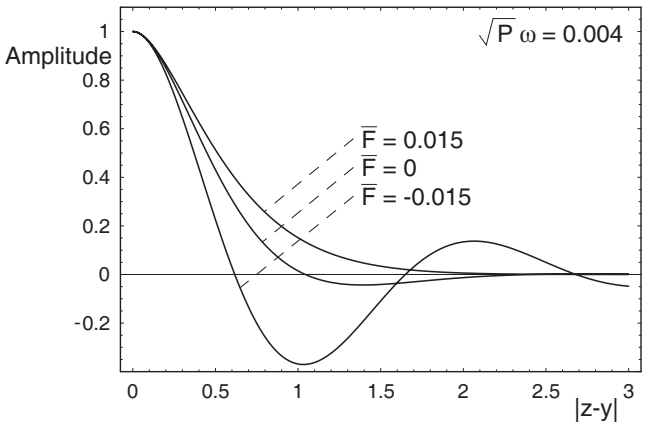

FIG. 6. Amplitude of vibration modes (normalized through division by the value at the origin) along the beam axis z (the point mass is located at y), for different values of prestress $\bar{F}$ and $\sqrt{P}\omega=0.004$.

It can be anticipated that the case of piecewise beam [Fig. 1(d)] is more interesting than the uniform case since (i) the dispersion diagrams exhibit several BGs (not only one as in the uniform case); (ii) the concentrated mass can be placed at different positions within the cell, thus providing different responses; and (iii) the vibration modes of the mass can be made more or less localized in the vicinity of the defect depending on the frequency (an effect shown in Ref. 7).

For a piecewise homogeneous beam, the Green's function is not available (although, in principle, it can be obtained analytically) and its expression would certainly be very involved, so that we prefer pursuing an approximate calculation, where a "sufficiently long," but finite, beam (seven elementary cells of length d in our examples) is solved, with a unit force applied at the central cell (the fourth cell in our examples).

Results pertinent to the seven-cell structure are reported in Fig. 7. Here the ranges of frequencies where localized modes associated with the concentrated mass *are possible* are reported as functions of the position y (normalized through division by d) of the mass in the central cell, for two levels of prestress, namely, $\bar{F}=0.025$ in Fig. 7(a) and $\bar{F}=0$ in Fig. 7(b).

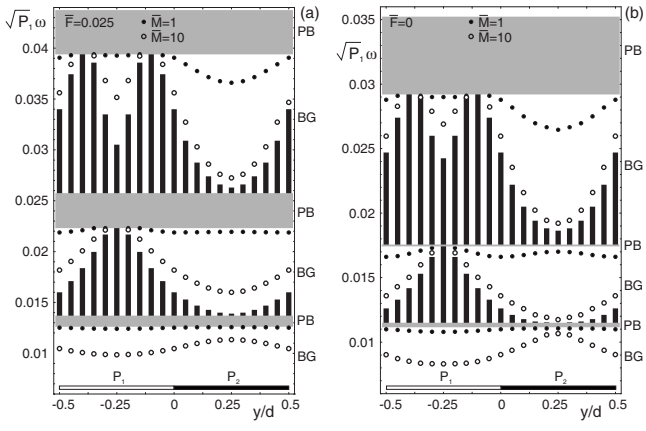

FIG. 7. Dimensionless frequency $\sqrt{P_1}\omega$ at which a localized mode connected to a concentrated point mass located at y [Fig. 1(d)] exists for $\bar{M}=1$ (black dots in the figure) and $\bar{M}=10$ (open circles) (the following values of constants have been taken: $P_2/P_1=0.1$, $l_1=l_2=d/2$, $r/d=0.015$, and $\bar{S}=0.0001$). (a) Tensile prestress: $\bar{F}=0.025$. (b) Null prestress: $\bar{F}=0$. BG denotes a band gap, while PB denotes a pass band (see Fig. 2). A black vertical segment in the BG zone indicates a frequency range where localized modes are not possible.

In Figs. 7(a) and 7(b), the first three BGs have been investigated, placing masses at discrete distances in multiples of $d/20$. Results depend on the dimensionless frequencies $\sqrt{P_1}\omega$ to generate localized modes associated with $\bar{M}=1$ (denoted with black dots) and 10 (denoted with black squares), where the dimensionless concentrated mass $\bar{M}$ is defined now with respect to the mass density and radius of inertia of part 1, namely,

$$\bar{M}=\frac{M}{2\rho_1 r_1}. \tag{23}$$

The black vertical segments crossing the BGs indicate frequency ranges where localized modes (and effective negative mass effects) *cannot be generated* by just inserting a single concentrated mass, being the displacement of the point of application of the unit force out of phase with respect to the force itself. We note that at certain locations y/d within the second and third BGs, these vertical segments cross the entire range (for instance, at $y=0.25d$, within the second BG, and at $y=0.2d$, $0.8d$, within the third BG), so that in these cases localized modes *cannot be obtained* for an applied finite and positive concentrated mass.

IV. CONCLUDING REMARKS

Prestress has been shown to deeply influence the vibrational response of elastic *periodic* systems, in particular, BG width (that can even be shrunk to zero), position (which shifts toward higher frequencies for tensile prestress), and effective negative mass effects. The prestress is therefore proposed as a candidate for controlling the dynamic response of active vibrational devices.

ACKNOWLEDGMENTS

This research has been supported by a Marie Curie Transfer of Knowledge Grant of the European Community VI Framework Programme under Contract No. MTKD-CT-2004-509809 and by PRIN Grant No. 2007YZ3B24 "Multiscale Problems with Complex Interactions in Structural Engineering" financed by the Italian Ministry of University and Research.

APPENDIX: BUCKLING LOAD OF A PIECEWISE CONSTANT STIFFNESS BEAM ON AN ELASTIC FOUNDATION

The buckling loads of a perfect beam with piecewise constant bending stiffness ($B_1 \neq B_2$) can be obtained by setting $\omega=0$ in Eqs. (1) and (6). Employing the normalization

$$\bar{F}_2=\bar{F}_1\frac{B_1}{B_2}\left(\frac{r_2}{r_1}\right)^2, \quad \bar{S}_2=\bar{S}_1\frac{B_1}{B_2}\left(\frac{r_2}{r_1}\right)^4,$$

in the governing equations, the buckling load of the structure $\bar{F}_1$ can be expressed in terms of B_2/B_1 at constant ratio r_2/r_1.

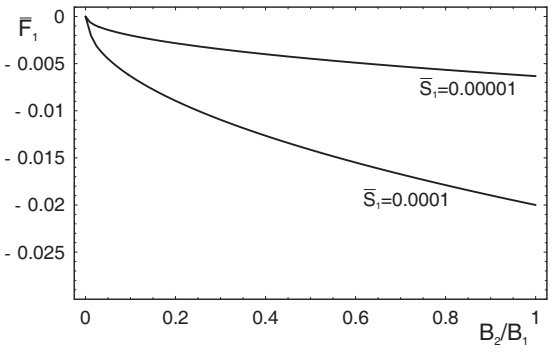

FIG. 8. Buckling load $\bar{F}_1$ of a beam on an elastic foundation with piecewise constant flexural stiffness, $B_1 \neq B_2$, for $\bar{S}_1=0.0001$ and $\bar{S}_1=0.00001$ ($r_1/d=r_2/d=0.015$ and $l_1=l_2=d/2$).

Some results are reported in Fig. 8 for two dimensionless foundation stiffnesses.

[1]References to phononic and photonic crystals can be found at http://www.phys.uoa.gr/phononics/PhononicDatabase.html and http://phys.lsu.edu/~jdowling/pbgbib.html.
[2]E. Yablonovitch, Phys. Rev. Lett. **58**, 2059 (1987).
[3]S. John, Phys. Rev. Lett. **58**, 2486 (1987).
[4]M. S. Kushwaha, P. Halevi, L. Dobrzynski, and B. Djafari-Rouhani, Phys. Rev. Lett. **71**, 2022 (1993).
[5]M. M. Sigalas and E. N. Economou, Solid State Commun. **86**, 141 (1993).
[6]M. D. Bacon, P. Dean, and J. L. Martin, Proc. Phys. Soc. London **80**, 174 (1962).
[7]A. B. Movchan and L. I. Slepyan, Proc. R. Soc. London, Ser. A **463**, 2709 (2007).
[8]J. B. Pendry, Phys. Rev. Lett. **85**, 3966 (2000).
[9]J. H. Page, A. Sukhovich, S. Yang, M. L. Cowan, F. Van Der Biest, A. Tourin, M. Fink, Z. Liu, C. T. Chan, and P. Sheng, Phys. Status Solidi B **241**, 3454 (2004).
[10]S. Yang, J. H. Page, Z. Liu, M. L. Cowan, C. T. Chan, and P. Sheng, Phys. Rev. Lett. **93**, 024301 (2004).
[11]X. Zhang and Z. Liu, Appl. Phys. Lett. **85**, 341 (2004).
[12]A.-C. Hladky-Hennion, J. Vasseur, B. Dubus, B. Djafari-Rouhani, D. Ekeom, and B. Morvan, J. Appl. Phys. **104**, 064906 (2008).
[13]P. Sheng, X. X. Zhang, Z. Liu, and C. T. Chan, Physica B **338**, 201 (2003).
[14]Z. Liu, C. T. Chan, and P. Sheng, Phys. Rev. B **71**, 014103 (2005).
[15]G. W. Milton and J. R. Willis, Proc. R. Soc. London, Ser. A **463**, 855 (2007).
[16]In sensor technology, active elements such as shape memory and piezoelectric inserts or patches are distributed periodically along the active device Refs. 17 and 18 in order to enable the filtering properties of the system; ways to tune the width of stop bands are described in Refs. 19–22.
[17]M. Ruzzene and A. Baz, J. Vibr. Acoust. **122**, 151 (2000).
[18]A. Baz, J. Vibr. Acoust. **123**, 472 (2001).
[19]X. Zhang, Z.-Q. Zhang, L.-M. Li, C. Jin, D. Zhang, B. Man, and B. Cheng, Phys. Rev. B **61**, 1892 (2000).
[20]C. Goffaux and J. P. Vigneron, Phys. Rev. B **64**, 075118 (2001).
[21]A. Khelief, P. A. Deymier, B. Djafari-Rouhani, J. O. Vasseur, and L. Dobrzynski, J. Appl. Phys. **94**, 1308 (2003).
[22]W. L. Liu, T.-J. Yang, and B.-Y. Gu, J. Phys.: Condens. Matter **16**, 4557 (2004).
[23]L. Cremer and H. O. Leilich, Arch. Elektr. Uebertrag. **7**, 261 (1953).
[24]J. W. Miles, J. Engrg. Mech. Div. **82**, 1 (1956).
[25]Y. K. Lin, Int. J. Mech. Sci. **4**, 409 (1962).
[26]D. J. Mead, J. Sound Vib. **40**, 19 (1975).
[27]D. J. Mead, J. Sound Vib. **190**, 495 (1996).
[28]D. Yu, Y. Liu, H. Zhao, G. Wang, and J. Qiu, Phys. Rev. B **73**, 064301 (2006).
[29]D. Yu, Y. Liu, H. Zhao, G. Wang, and J. Qiu, J. Appl. Phys. **100**, 124901 (2006).
[30]D. Bigoni and A. B. Movchan, Int. J. Solids Struct. **39**, 4843 (2002).
[31]A. B. Movchan and S. Guenneau, Phys. Rev. B **70**, 125116 (2004).
[32]C. G. Poulton, S. Guenneau, and A. B. Movchan, Phys. Rev. B **69**, 195112 (2004).
[33]The recent long-wave asymptotic analysis of a layer with periodic mass density (Ref. 34), coating an elastic half space, has revealed some of the effects addressed in the present article. Previous contributions Refs. 35 and 36 have highlighted the strong effects related to prestress in homogeneous elastic solids, where band gaps and localized modes are excluded. A unidimensional model, limited to longitudinal wave propagation in an elastic prestressed material, has been considered by Parnell (Ref. 37), showing effects in agreement to those evidenced in the present article.
[34]D. Bigoni, M. Gei, and A. B. Movchan, J. Mech. Phys. Solids **56**, 2494 (2008).
[35]D. Bigoni and D. Capuani, J. Mech. Phys. Solids **53**, 1163 (2005).
[36]D. Bigoni, D. Capuani, P. Bonetti, and S. Colli, Comput. Methods Appl. Mech. Eng. **196**, 4222 (2007).
[37]W. J. Parnell, IMA J. Appl. Math. **72**, 223 (2007).
[38]K. F. Graff, *Wave Motion in Elastic Solids* (Oxford University Press, New York, 1975).
[39]V. V. Zalipaev *et al.* (Ref. 40) developed an asymptotic approach to longitudinal vibrations of an elastic beam (without prestress) containing defects at its boundary and found that the "effective boundary conditions" for the first-order asymptotic problem are either of Dirichlet type (the boundary of the thin body is clamped), Robin type (stress and displacement satisfy an elastic constitutive equation), or Neumann type (the boundary, strongly damaged, becomes traction-free).
[40]V. V. Zalipaev, A. B. Movchan, and I. S. Jones, Q. J. Mech. Appl. Math. **60**, 457 (2007).
[41]S. Nudehi, R. Mukherjee, and S. W. Shaw, J. Dyn. Syst., Meas., Control **128**, 278 (2006).
[42]C. Gui, R. Legtenberg, H. A. C. Tilmans, J. H. J. Fluitman, and M. Elwenspoek, J. Microelectromech. Syst. **7**, 122 (1998).
[43]V. Kaajakari, T. Mattila, A. Oja, and H. Seppä, J. Microelectromech. Syst. **13**, 715 (2004).
[44]We refer to "effective negative mass effects" as the exponentially decaying propagation modes that can be found in elastic systems in the way addressed in Ref. 15.
[45]R. Feynman, *The Feynman Lectures on Physics* (Addison-Wesley, Reading, MA, 1965), Vol. 2.
[46]S. P. Timoshenko, W. Weaver, and D. H. Young, *Vibration Problems in Engineering* (Wiley, New York, 1974).
[47]T. G. Chondros, A. D. Dimarogonas, and J. Yao, J. Sound Vib. **215**, 17 (1998).
[48]In the case of a *homogeneous* beam on an elastic foundation, all quantities introduced in Eqs. (1), (4), and (5) are constant along axis z. Therefore, the dispersion equation (3) simplifies to

$$P\omega^2 = (kr)^4 + \bar{F}(kr)^2 + \bar{S},$$

possessing the following features: (i) In the long-wavelength limit ($kr \to 0$), ω satisfies the cutoff limit $P\omega_0^2=\bar{S}$. (ii) The frequency is monotonic for tensile (or null) prestress, $\bar{F} \geqslant 0$, so that $\omega_{\min}=\omega_0$ in this case. (iii) For a compressive prestress, $\bar{F}<0$, the function of the above equation displays a minimum such that $P\omega_{\min}^2=\bar{S}-\bar{F}^2/4$ and, consequently, buckling ($\omega_{\min}=0$) occurs at $\bar{F}_{\text{buckl}}=-2\sqrt{\bar{S}}$ with $k_{\text{buckl}}r=\bar{S}^{1/4}$.
[49]$\Phi(x)=0.6272x^2-1.04533x^3+4.5948x^4-9.9736x^5+20.2948x^6-33.0351x^7+47.1063x^8-40.7556x^9+19.6x^{10}$.